



1 **Particle acidity and sulfate production during severe haze events in China**
2 **cannot be reliably inferred by assuming a mixture of inorganic salts**

3
4 Gehui Wang^{1,2,3}, Fang Zhang^{4,5}, Jianfei Peng^{5,6}, Lian Duan^{5,7}, Yuemeng Ji^{5,8}, Wilmarie
5 Marrero-Ortiz⁵, Jiayuan Wang², Jianjun Li², Can Wu², Cong Cao², Yuan Wang⁹, Jun Zheng¹⁰,
6 Jeremiah Secrest⁵, Yixin Li⁵, Yuying Wang^{4,5}, Hong Li¹¹, Na Li^{5,12}, and Renyi Zhang^{5,6*}

7
8 ¹ Key Laboratory of Geographic Information Science of the Ministry of Education, School of
9 Geographic Sciences, East China Normal University, Shanghai 200241, China

10 ² State Key Laboratory of Loess and Quaternary Geology, Institute of Earth Environment, China
11 Academy of Sciences, Xi'an 710061, China

12 ³ Center for Excellence in Regional Atmospheric Environment, Institute of Urban Environment,
13 Chinese Academy of Science, Xiamen, China

14 ⁴ Beijing Normal University, Beijing 100875, China

15 ⁵ Departments of Atmospheric Sciences and Chemistry, Texas A&M University, College Station,
16 TX, 77843, USA

17 ⁶ State Key Joint Laboratory of Environmental Simulation and Pollution Control, College of
18 Environmental Sciences and Engineering, Peking University, Beijing 100871, China

19 ⁷ East China University of Science and Technology, Shanghai, China

20 ⁸ School of Environmental Science and Engineering, Institute of Environmental Health and
21 Pollution, Control, Guangdong University of Technology, Guangzhou 510006, China

22 ⁹ Jet Propulsion Laboratory, California Institute of Technology, Pasadena, CA 91125, USA

23 ¹⁰ Jiangsu Key Laboratory of Atmospheric Environment Monitoring and Pollution Control,
24 Nanjing University of Information Science & Technology, Nanjing 210044, China

25 ¹¹ State Key Laboratory of Environmental Criteria and Risk Assessment, Chinese Research
26 Academy of Environmental Sciences, Beijing 100012, China

27 ¹² Key Laboratory of Songliao Aquatic Environment, Jilin Jianzhu University, Changchun,
28 130118, China

29
30
31
32
33 *Corresponding author:

34 Prof. Renyi Zhang, E-mail: renyi-zhang@tamu.edu

35



36 **Abstract:** Atmospheric measurements showed rapid sulfate formation during severe haze
37 episodes in China, with fine particulate matter (PM) consisting of a multi-component mixture
38 that is dominated by organic species. Several recent studies using the thermodynamic model
39 estimated the particle acidity and sulfate production rate, by treating the PM exclusively as a
40 mixture of inorganic salts dominated by ammonium sulfate and neglecting the effects of organic
41 compounds. Noticeably, the estimated pH and sulfate formation rate during pollution periods in
42 China were highly conflicting among the previous studies. Here we show that a particle mixture
43 of inorganic salts adopted by the previous studies does not represent a suitable model system and
44 that the acidity and sulfate formation cannot be reliably inferred without accounting for the
45 effects of multi-aerosol compositions during severe haze events in China. Our laboratory
46 experiments show that SO₂ oxidation by NO₂ with NH₃ neutralization on fine aerosols is
47 dependent on the particle hygroscopicity, phase-state, and acidity. Ammonium sulfate and oxalic
48 acid seed particles exposed to vapors of SO₂, NO₂, and NH₃ at high relative humidity (RH)
49 exhibit distinct size growth and sulfate formation. Aqueous ammonium sulfate particles exhibit
50 little sulfate production because of high acidity, in contrast to aqueous oxalic acid particles with
51 significant sulfate production because of low acidity. Our field measurements demonstrate
52 significant contribution of water-soluble organic matter to fine PM in China and indicate that the
53 use of oxalic acid in laboratory experiments is representative of ambient organic dominant
54 aerosols. While the particle acidity cannot be accurately determined from field measurements or
55 calculated using the thermodynamic model, our results reveal that the pH value of ambient
56 organics-dominated aerosols is sufficiently high to promote efficient SO₂ oxidation by NO₂ with
57 NH₃ neutralization under polluted conditions in China.

58

59



60 1. Introduction

61 Atmospheric measurements have demonstrated rapid sulfate production during severe haze
62 events in China (Guo et al., 2014; Wang et al., 2014; Zhang et al., 2015; Cheng et al., 2016;
63 Wang et al., 2016). For example, Wang et al. (2016) showed that during pollution episodes in
64 Xi'an of China the SO_4^{2-} mass concentration increased markedly from less than 10, 10-20, to
65 greater than $20 \mu\text{g m}^{-3}$, with the corresponding increases in the mean $\text{PM}_{2.5}$ mass concentrations
66 from 43, 139, to $250 \mu\text{g m}^{-3}$ from clean, transition, to polluted periods, respectively. Among the
67 $\text{PM}_{2.5}$ species in Xi'an, organic matter (OM), nitrate (NO_3^-), and SO_4^{2-} were most abundant, with
68 the mass fractions of 55%, 14%, and 14%, respectively, during the polluted period. In addition,
69 the work by Wang et al. (2016) demonstrated that the molar ratio of SO_4^{2-} to SO_2 , which reflects
70 sulfur partitioning between the particle and gas phases, exhibited an exponential increase with
71 relative humidity (RH), with the values of less than 0.1 at $\text{RH} < 20\%$ to 1.1 at $\text{RH} > 90\%$ in
72 Xi'an. Similar evolutions in SO_4^{2-} mass concentrations and the molar ratio of SO_4^{2-} to SO_2 were
73 shown during the pollution development in Beijing (Sun et al., 2013; Wang et al., 2014; Wang et
74 al., 2016). The rapid sulfate formation measured in China could not be explained by current
75 atmospheric models and suggested missing sulfur oxidation mechanisms (Wang et al., 2014).
76 Typically, high sulfate levels during haze events in China occurred concurrently with elevated
77 RH, NO_x , and NH_3 (Wang et al., 2014; Zhang et al., 2015; Wang et al., 2016), implicating an
78 aqueous sulfur oxidation pathway. On the basis of complementary field and experimental
79 measurements, Wang et al. (2016) concluded that the aqueous oxidation of SO_2 by NO_2 is key to
80 efficient sulfate formation, but is only feasible under two atmospheric conditions, i.e., on fine
81 aerosols with high RH and NH_3 neutralization or under cloud conditions.

82 Several recent studies estimated the particle acidity and aqueous sulfate production during



83 severe haze events in China using the thermodynamic model (Cheng et al., 2016; Guo et al.,
84 2017; Liu et al., 2017). For example, Cheng et al. (2016) estimated a pH range of 5.4 to 6.2 using
85 a thermodynamic model (ISORROPIA-II) in Beijing. On the basis of their estimated pH and the
86 previous experimental rates of SO₂ oxidation by NO₂ and the Henry's Law constants for sulfur
87 dioxide (SO₂), bisulfite (HSO₃⁻), and sulfite (SO₃²⁻) from the literature (Lee and Schwartz, 1983;
88 Clifton et al., 1988; Seinfeld and Pandis, 2006), the authors derived a sulfate production rate and
89 concluded that reactive nitrogen chemistry in aerosol water explained the sulfate formation
90 during polluted periods in Beijing. In contrast, other recent studies by Guo et al. (2017) and Liu
91 et al. (2017) adopted the similar method as Cheng et al. (2016), but reported significantly
92 different values of pH and the sulfate formation rates by the aqueous SO₂ oxidation by NO₂ in
93 China. Those two later studies determined a pH range of 3.0-4.9 and suggested that fine particles
94 were moderately acidic and the aqueous SO₂ oxidation by NO₂ was unimportant during severe
95 wintertime haze periods in China.

96 In this article, we conducted laboratory measurements of the hygroscopicity for oxalic acid
97 particles and particle growth of ammonium sulfate particles upon exposure to SO₂, NO₂, and
98 NH₃ at high RH conditions, in order to evaluate the dominant factors regulating the aqueous
99 oxidation of SO₂ by NO₂. In addition, field measurements of chemical compositions of water-
100 soluble fraction for fine PM (including oxalic acid) in Beijing, Hebei Province, and Xi'an of
101 China were performed during the winter haze episodes, showing significantly enriched water-
102 soluble organic matter (WSOM). The implications for the multi-aerosol chemical compositions
103 on the pH value and sulfate production during winter pollution periods in China are discussed.

104 2. Methods

105 2.1 Aqueous phase oxidation of SO₂ by NO₂ in an environmental chamber



106 The experimental method using the environmental chamber has been discussed elsewhere
107 (Wang et al., 2016), and here we only provide a brief description. The aqueous SO₂ oxidation
108 experiments was conducted by exposing size-selected (NH₄)₂SO₄ seed particles to different
109 levels of SO₂, NO₂, and NH₃ at variable RH conditions in a 1 m³ Teflon reaction chamber
110 covered with aluminum foil. A differential mobility analyzer (DMA) equipped with a
111 condensation particle counter (CPC) was used to measure the particle growth in diameter, in
112 order to determine sulfate formation on seeded particles (Wang et al., 2016).

113 2.2 Measurement of hygroscopic growth factor of oxalic acid

114 Hygroscopic growth factor (HGF) of oxalic acid was measured according to the method
115 previously discussed (Khalizov et al., 2009; Pagels et al., 2009). Briefly, a hygroscopicity
116 tandem differential mobility analyzer (HTDMA) coupled to a condensation particle counter
117 (CPC, TSI 3762) was used for the HGF measurement. Size-selected oxalic acid particles with the
118 dry diameter of 100 nm were exposed to increasing RH from 8% to 92% with a step range from
119 1%-10%. HGF is defined as the ratio of oxalic acid particle diameter (D_p) measured by the
120 second DMA at an elevated RH to the initial diameter ($D_0 = 100$ nm) of the particles selected by
121 the first DMA at the dry conditions of RH = 8% (Peng et al., 2016).

122 2.3 Chemical composition of PM_{2.5} in Beijing, Hebei Province, and Xi'an, China

123 PM_{2.5} samples were collected onto pre-baked (450°C for 6 hr) quartz fiber filter by using a
124 high-volume air sampler with an airflow rate of 1.03 m³ min⁻¹. The sample collection in Xi'an
125 was performed on the roof of a three-story building in the urban center with a 1-hour interval for
126 each sample during the winter of 2012 (Wang et al., 2016). The sample collection in Beijing was
127 conducted during the winter of 2016 on the roof of a four-story building on the campus of China
128 Research Academy of Environmental Sciences, which is located at the northern part of Beijing.



129 The PM_{2.5} samples in Hebei Province were collected during the winter of 2016 on the roof of a
130 three-story building on the campus of the Institute of Hydrology and Environmental Geology,
131 which is located in Zhengding County of Hebei Province. Both sample collections in Beijing and
132 Hebei Province were performed on a day/night basis. After collection, all samples were sealed
133 individually in an aluminum foil bag and stored in a freezer below -18°C prior to analysis.

134 The detailed procedures for the analysis of inorganic ions and water-soluble organic matter
135 (WSOM) in aerosols have been reported elsewhere (Wang et al., 2009; Wang et al., 2010; Wang
136 et al., 2017). Briefly, one part of the filter sample (area about 5 cm²) was divided into several
137 pieces, extracted with Milli-Q pure water, and determined for WSOM and inorganic ions by
138 using Shimadzu TOC-L CPH analyzer and Dionex-600 ion chromatography, respectively.
139 Oxalic acid in PM_{2.5} was analyzed according to Wang et al. (2002) and Cheng et al. (2015). One
140 part of the filter sample was extracted with Milli-Q water, concentrated to dryness, and reacted
141 with 14% BF₃/butanol at 100°C for 1 hr. After the reaction, the derivatized sample was extracted
142 with hexane for three times and concentrated into 1 mL. Oxalic acid in the samples was
143 identified by gas chromatography–mass spectrometry (GC–MS) and quantified by gas
144 chromatography (Agilent GC7890A).

145 **3. Results**

146 **3.1 Aqueous oxidation of SO₂ by NO₂ with NH₃ neutralization**

147 We first evaluated the factors controlling the aqueous phase oxidation of SO₂ by NO₂ using
148 the environmental chamber method. The evolution in the size of ammonium sulfate particles
149 after exposure to SO₂, NO₂, and NH₃ at different RH and SO₂ levels is shown in Figure 1. In our
150 experiments, monodisperse particles with the initial dry particle size ranging from 50 to 70 nm
151 were selected for the exposure, and two different SO₂ concentrations (37.5 and 375 parts per



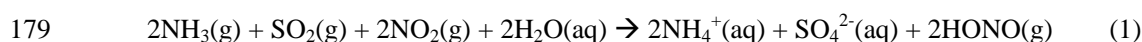
152 billions or ppb) were used. RH was maintained at a level of 80-98%, above the deliquescence
153 point (79%) of ammonium sulfate (Qiu and Zhang, 2013) to ensure aqueous particles. As is
154 shown in Figure 1, the size of $(\text{NH}_4)_2\text{SO}_4$ particles remains nearly invariant (within the
155 experimental uncertainty) after exposure to SO_2 , NO_2 , and NH_3 . A 10-fold increase in the SO_2
156 concentration has little effect on the growth of $(\text{NH}_4)_2\text{SO}_4$ particles. These results illustrate that
157 sulfate production is insignificant and SO_2 cannot be efficiently oxidized by NO_2 in the presence
158 of NH_3 on aqueous ammonium sulfate particles. The measurement of negligible growth for
159 $(\text{NH}_4)_2\text{SO}_4$ particles exposed to SO_2 , NO_2 , and NH_3 at high RH is in contrast to the previous
160 work by Wang et al. (2016), which showed large size growth and significant sulfate production
161 for oxalic acid particles with NH_3 neutralization and under high RH conditions.

162 To gain an insight into such a difference in the size growth between $(\text{NH}_4)_2\text{SO}_4$ and oxalic
163 acid particles, we measured the hygroscopic growth of oxalic acid particles. Figure 2 displays the
164 measured hygroscopic growth factor (HGF) of oxalic acid, showing an exponential increase with
165 an increase in RH. The measured HGF value is close to unity at $\text{RH} < 40\%$ and increases from
166 1.1 at $\text{RH} = 60\%$ to 1.5 at $\text{RH} = 90\%$. Our measured HGF for oxalic acid is consistent with the
167 previous studies by Prenni et al. (2001) and Mikhailov et al. (2009). On the other hand, another
168 earlier experimental study showed little growth for oxalic acid particles under high RH
169 conditions (Peng et al., 2001). The measurements of HGF also provide information on the
170 particle phase-state. As evident from Figure 2, oxalic acid particles mainly exist in a non-
171 aqueous phase at $\text{RH} < 40\%$ but in the aqueous phase at $\text{RH} > 60\%$.

172 Our present experiments of aqueous oxidation of SO_2 by NO_2 were performed at similar
173 conditions as those by Wang et al. (2016), i.e., with comparable concentrations for SO_2 , NO_2 ,
174 and NH_3 and in the same phase-state (aqueous) for the particles. On the other hand, the particle



175 acidity is clearly distinct between the two studies. Our present experiment is characterized by a
176 lower pH value, since ammonium sulfate is rather acidic. For example, the pH value of 0.1M
177 $(\text{NH}_4)_2\text{SO}_4$ solution is 5.5. The overall aqueous reaction between SO_2 and NO_2 in the presence of
178 NH_3 is suggested as the following (Wang et al., 2016),



180 Since the solubility of SO_2 and NO_2 decreases markedly with increasing particle acidity
181 (Seinfeld and Pandis, 2006; Zhang et al., 2015), the heterogeneous reaction between SO_2 and
182 NO_2 is prohibited on acidic $(\text{NH}_4)_2\text{SO}_4$ particles. On the other hand, under the experimental
183 conditions by Wang et al. (2016), the heterogeneous reaction between oxalic acid and NH_3
184 occurred on aqueous particles in the presence of NH_3 , yielding ammonium oxalate. The
185 ammonium oxalate is less acidic than ammonium sulfate. The pH value of 0.1 M ammonium
186 oxalate is 6.5, which is one unit higher than that of ammonium sulfate. As a result, SO_2 readily
187 dissolves into aqueous ammonium oxalate particles and is oxidized by NO_2 into SO_4^{2-} , which is
188 consequently neutralized by NH_3 to produce $(\text{NH}_4)_2\text{SO}_4$. The resulting aqueous ammonium
189 oxalate/ $(\text{NH}_4)_2\text{SO}_4$ particles exhibit a lower acidity than that of $(\text{NH}_4)_2\text{SO}_4$ particles, responsible
190 for a significant growth in the dry particle size and sulfate formation for the previous
191 experiments by Wang et al. (2016).

192 Hence, the experimental studies of our present work and that by Wang et al. (2016) reveal
193 that sulfate production on fine particles is dependent on several factors, including the particle
194 hygroscopicity, phase-state, acidity, and RH, in addition to the gaseous concentrations of SO_2 ,
195 NO_2 , and NH_3 . These experimental results indicate that the acidity and sulfate formation are
196 distinct for organic seed and ammonium sulfate seed particles. While oxidation of SO_2 by NO_2
197 on aqueous $(\text{NH}_4)_2\text{SO}_4$ particles does not represent a viable mechanism because of a higher



198 acidity, significant sulfate production occurs on oxalic acid particles because of a lower acidity.

199 **3.2 Field measurements of WSOM in China**

200 Atmospheric measurements have shown that the occurrence of severe haze episodes in
201 China is accompanied with high RH conditions and PM_{2.5} particles consist of large amounts of
202 secondary organic and inorganic compounds. We present additional field measurements of the
203 chemical composition of PM_{2.5} in Beijing, Hebei Province, and Xi'an of China. Figure 3 shows
204 that the wintertime PM_{2.5} samples collected at the three locations. It is evident that WSOM is
205 considerably enriched and their concentrations are comparable to those of the total inorganic ions
206 (Figure 3a and b). For example, the mass concentration of WSOM ranges from 10 to 60 $\mu\text{g m}^{-3}$
207 in Beijing and Hebei Province during the winter of 2016 and from 10 to 180 $\mu\text{g m}^{-3}$ in Xi'an
208 during the winter of 2012 (Figure 3c and d, respectively). In addition, the variation of WSOM
209 displays a temporal pattern similar to that of oxalic acid, with a linear correlation coefficient of
210 0.79, 0.88 and 0.72 in Beijing, Hebei Province, and Xi'an, respectively (Figure 3e and f). The
211 mass concentration of oxalic acid in fine PM during the haze episodes is about 500 ng m^{-3} in
212 Beijing and Hebei Province (Figure 3e) and more than 2000 ng m^{-3} in Xi'an (Figure 3f). Hence,
213 our field measurements indicate that oxalic acid represents one of the most abundant WSOM in
214 the aerosol-phase. Oxalic acid, a secondary product formed from the photochemical oxidation of
215 volatile organic compounds, has been also shown to exist with large abundance in China (Wang
216 et al., 2012; Cheng et al., 2013; Meng et al., 2014; Kawamura and Bikkina, 2016). In addition,
217 the previous field measurements also revealed that WSOM in China is not only enriched in
218 carboxylic acids (including oxalic acid) but also in other organic species, including carbonyls,
219 amines, and water-soluble nitrogen-containing organic compounds (Wang et al., 2010, 2013;
220 Zheng et al., 2015; Yao et al., 2016; Liu et al., 2017). The dominant organic acids and bases



221 indicate that haze particles in China are multi-component in nature and the estimations of the
222 particle acidity (or pH) and the sulfate production rate need to take into account of the effects of
223 organic species, in addition to inorganic ions.

224 **4. Discussions**

225 Several recent studies using the thermodynamic models (Wexler and Clegg, 2002;
226 Fountoukis and Nenes, 2007) estimated the particle acidity and sulfate production during
227 pollution episodes in China (Cheng et al., 2016; Guo et al., 2017; Liu et al., 2017). Those
228 previous studies treated the PM exclusively as a mixture of inorganic salts dominated by
229 ammonium sulfate and neglected the effects due to the presence of organic compounds.
230 Apparently, the conclusions by those modeling studies hinge on the validity of several critical
231 assumptions in their analyses, including the application of the thermodynamic model, the
232 accuracy in determining the aerosol water content (AWC), and the applicability of the earlier
233 experimental measurements for the aqueous oxidation of SO₂ by NO₂ to atmospheric conditions.

234 Estimation of the pH values using the thermodynamic models is typically of considerable
235 uncertainty, because of several intricate difficulties. For example, the ISORRPIA-II model
236 includes two modes, i.e., metastable (aerosols are assumed to be in the liquid-phase only and
237 may reach supersaturation) and stable (aerosols are assumed in the liquid- and solid phases that
238 are in equilibrium) (Guo et al., 2017). Since the thermodynamic model is established on the basis
239 of the equilibrium principles, its application to non-equilibrium conditions needs to be rigorously
240 assessed. Also, the phase (e.g., liquid, amorphous, or crystalline) and mixing state of ambient
241 aerosols are highly complex because of the presence of multi-component organic and inorganic
242 species (Qiu and Zhang, 2013; Zhang et al., 2015), inevitably rendering high uncertainty in the
243 thermodynamic calculations.



244 Guo et al. (2017) suggested that the pH predictions using the metastable mode would be
245 more reliable than that using the stable mode, on the basis of model evaluation from measured
246 and predicted NO_3^- and NH_4^+ during the winter of 2012 in Xi'an. Figure 4 compares the
247 concentrations of NH_3 (g) and aerosol species predicted by ISORROPIA-II with the field
248 measurements under the metastable and stable modes in Xi'an during the winter of 2012. As
249 evident in Figure 4a and b, NH_3 predicted is similar to the measured value with the metastable or
250 stable mode. Furthermore, the predicted concentrations of NO_3^- and NH_4^+ using both the
251 metastable and stable modes are nearly identical (Figure 4c-f). Guo et al. (2017) only compared
252 the liquid NH_4^+ and NO_3^- predicted by the model with the field measured aerosols composed of
253 both liquid and solid compounds, and their predicted concentrations were lower than those of the
254 measurements (see Figure S1 in Guo et al, 2017). As a result, their statement that pH prediction
255 with the metastable mode would be more reliable than that with the stable mode was unjustified.
256 Noticeably, the pH values estimated by the ISORROPIA-II model under the two modes are
257 significantly different, with the values of 4.57 ± 0.40 under the metastable mode and 6.96 ± 1.33
258 under the stable mode. Most recently, it was suggested that the large discrepancy in predicting
259 pH is attributable to the differences in the model assumptions (Song et al., 2018).

260 In addition, the pH estimation by the thermodynamic model is highly dependent on the ratio
261 of the concentration of hydrogen ions in the liquid-phase to AWC. Guo et al. (2017) and Liu et al.
262 (2017) assumed negligible particle water associated with the organic aerosol mass. Such an
263 assumption is clearly invalid since aerosols typically contain a large portion of WSOM in China
264 (Fig. 3), including organic nitrogen species (Wang et al., 2010, 2013) and acids (Wang et al.,
265 2006, 2009, 2010). Also, organic acids engage in particle-phase reactions with the basic species
266 (i.e., NH_3 and amines), significantly enhancing the particle hygroscopicity and reducing the



267 acidity (Gomez-Hernandez et al., 2016). In addition, because of their strong basicity and high
268 abundance, amines likely play a key role in reducing the particle-acidity in China (Wang et al.,
269 2010a, b; Qiu et al., 2011; Qiu and Zhang, 2012; Dong et al., 2013; Zheng et al., 2015; Yao et al.,
270 2016; Liu et al., 2017). Consequently, the acidity for organics-dominated aerosols is
271 considerably different from that of ammonium sulfate aerosols, as demonstrated in our
272 experimental results. While effort has been made to account for the effects of organic species on
273 the aerosol properties (Clegg et al., 2013), the available thermodynamic models are still
274 inadequate in representing complex multi-component aerosols. An inconsistency of the
275 ammonium–sulfate ratios using the thermodynamic models was identified in the eastern US, also
276 suggesting a possible role for organic species (Silvern et al., 2017).

277 Furthermore, the chemical mechanism leading to the aqueous conversion of SO₂ to sulfate
278 by NO₂ is not well understood. The previous modeling studies adopted the aqueous reaction rate
279 constants previously measured (Lee and Schwartz, 1983; Clifton et al., 1988), while the
280 applicability of the earlier experimental studies to atmospheric conditions is uncertain. For
281 example, Lee and Schwartz (1983) examined the oxidation of S(IV) by NO₂ in the liquid phase
282 by flowing gaseous NO₂ through a NaHSO₃ solution at a constant pH by regulating NaOH and
283 determined the rate constant of $1.4 \times 10^5 \text{ M}^{-1} \text{ s}^{-1}$ at pH = 5 and with a lower limit of $2 \times 10^6 \text{ M}^{-1} \text{ s}^{-1}$
284 at pH = 5.8 and 6.4 from measuring the electrical conductivity of the solution. Clifton et al.
285 (1988) measured the rate constant for the reaction of NO₂ with S(IV) over the pH range of 5.3–13,
286 by producing NO₂ from irradiation of NaNO₂ and N₂O solutions and mixing with Na₂SO₃
287 solutions, and obtained the second-order rate constant of 1.24×10^7 and $2.95 \times 10^7 \text{ M}^{-1} \text{ s}^{-1}$ from
288 the decay of NO₂ monitored by absorption spectroscopy. The results of the measured rate
289 constants between the two earlier experimental measurements differed by 1–2 orders of



290 magnitude (Lee and Schwartz, 1983; Clifton et al., 1988). Also, both kinetic experiments
291 employed bulk solutions and did not account for the gaseous uptake process (Lee and Schwartz,
292 1983; Clifton et al., 1988).

293 Wang et al. (2016) obtained the SO₂ uptake coefficient for sulfate production from
294 combined field measurements and laboratory experiments, and their laboratory experiments
295 using aqueous oxalic acid particles reproduced the rapid sulfate production measured under
296 polluted ambient conditions. The results of the SO₂ uptake coefficients determined by Wang et al.
297 (2016) are consistent with the modeling studies in quantification of the sulfate formation using
298 atmospheric models in China (e.g., Wang et al., 2014). On the other hand, Liu et al. (2017)
299 invoked the experimental work by Hung et al. (2015) as a plausible cause for rapid SO₂
300 oxidation by O₂ in the absence of photochemistry, but without noting the high acidity as a
301 necessary condition in that experimental work (i.e., pH ≤ 3). Most recently, Li et al. (2018)
302 suggested an indirect mechanism of SO₂ oxidation by NO₂ via HONO/NO₂⁻ produced in fast-
303 hydrolytic disproportionation of NO₂ on the surface of NaHSO₃ aqueous microjets. In addition,
304 another recent theoretical work by Zhang et al. (2018) indicated that under weakly acidic and
305 neutral conditions (pH ≤ 7) the oxidation of HOSO₂⁻ by dissolved NO₂ is a self-sustaining
306 process, where the produced *cis*-HONO, HSO₄⁻ and H₂SO₄ promote the tautomerization from
307 HSO₃⁻ to HOSO₂⁻ as the catalysts.

308 5. Conclusions

309 In this paper we have presented experimental measurements of the growth of ammonium
310 sulfate seed particles exposed to vapors of SO₂, NO₂, and NH₃ at variable RH, the HGF of oxalic
311 acid particles, and field measurements of WSOM for PM_{2.5} during the severe haze events in
312 Beijing, Hebei Province, and Xi'an of China. Our experimental results reveal that sulfate



313 production on fine particles is dependent on the particle hygroscopicity, phase-state, and acidity,
314 as well as RH. The acidity and sulfate formation for ammonium sulfate seed particles are distinct
315 from those of oxalic acid seed particles. Aqueous ammonium sulfate particles show negligible
316 growth because of low pH, in contrast to aqueous oxalic acid particles with significant dry-size
317 increase and sulfate formation because of high pH. In addition, our atmospheric measurements
318 show significant concentrations of WSOM (including oxalic acid) in fine PM, indicating multi-
319 component haze particles in China. Our results reveal that a particle mixture of inorganic salts
320 adopted by the previous studies using the thermodynamic model does not represent a suitable
321 model system and that the particle acidity and aqueous sulfate formation rate cannot be reliably
322 inferred without accounting for the effects of multi-chemical compositions during severe haze
323 events in China. Our combined experimental and field measurements corroborate the earlier
324 finding that sulfate production via the particle-phase reaction involving SO₂ and NO₂ with NH₃
325 neutralization occurs efficiently on organics-dominated aerosols (Wang et al., 2016) but are in
326 contradiction to the most recent studies using the thermodynamic model (Guo et al., 2017; Liu et
327 al., 2017).

328 In conclusion, while the particle acidity or pH cannot be accurately determined from
329 atmospheric field measurements or calculated using the thermodynamic models, our combined
330 experimental and field results provide the compelling evidence that the pH value of ambient
331 organics-dominated particles is sufficiently high to promote SO₂ oxidation by NO₂ with NH₃
332 neutralization under polluted conditions in China.

333 **Acknowledgements**

334 Financial support for this work was provided by National Key R&D Plan (Quantitative
335 Relationship and Regulation Principle between Regional Oxidation Capacity of Atmospheric and



336 Air Quality (No. 2017YFC0210000), the China National Natural Science Funds for
337 Distinguished Young Scholars (No.41325014), the program from National Nature Science
338 Foundation of China (No. 41773117). This work was also supported by the Robert A. Welch
339 Foundation (Grant A-1417) W.M.-O. was supported by the National Science Foundation
340 Graduate Research Fellowship Program.
341

342 **References**

- 343 Cheng, C., Wang, G., Zhou, B., Meng, J., Li, J., Cao, J., and Xiao, S.: Comparison of
344 dicarboxylic acids and related compounds in aerosol samples collected in Xi'an, China
345 during haze and clean periods, *Atmospheric Environment*, 81(0), 443-449, 2013.
- 346 Cheng, C., Wang, G., Meng, J., Wang, Q., Cao, J., Li, J., and Wang, J.: Size-resolved airborne
347 particulate oxalic and related secondary organic aerosol species in the urban atmosphere of
348 Chengdu, China, *Atmospheric Research*, 161–162, 134-142, 2015.
- 349 Cheng, Y., Zheng, G., Wei, C., Mu, Q., Bo Zheng, Wang, Z., Gao, M., Zhang, Q., He, K.,
350 Carmichael, G., Pöschl, U., and Su, H.: Reactive nitrogen chemistry in aerosol water as a
351 source of sulfate during haze events in China, *Science Advances*, 2, e1601530, 2016.
- 352 Clegg, S.L., Qiu, C., Zhang, R.: The deliquescence behaviour, solubilities, and densities of
353 aqueous solutions of five methyl- and ethyl-aminium sulphate salts, *Atmospheric*
354 *Environment*, 73, 1-14, 2013.
- 355 Clifton, C. L., Altstein, N., and Huie, R. E.: Rate constant for the reaction of nitrogen dioxide
356 with sulfur(IV) over the pH range 5.3-13, *Environmental Science & Technology*, 22, 586-
357 589, 1988.
- 358 Dong, X. L., Liu, D. M., and Gao, S. P.: Seasonal variations of atmospheric heterocyclic
359 aromatic amines in Beijing, China, *Atmospheric Research*, 120, 287-297, 2013.
- 360 Fountoukis, C., and Nenes, A.: ISORROPIA II: A computationally efficient thermodynamic
361 equilibrium model for K^+ - Ca^{2+} - Mg^{2+} - NH_4^+ - Na^+ - SO_4^{2-} - NO_3^- - Cl^- - H_2O aerosols, *Atmospheric*
362 *Chemistry and Physics*, 7, 4639-4659, 2007.
- 363 Gomez-Hernandez, M., McKeown, M., Secret, J., Marrero-Ortiz, W., Lavi, A., Rudich, Y.,
364 Collins, D. R., and Zhang, R.: Hygroscopic characteristics of alkylaminium carboxylate
365 Aerosols, *Environmental Science & Technology*, 50, 2292-2300, 2016.
- 366 Guo, H., Weber, R. J., and Nenes, A.: High levels of ammonia do not raise fine particle pH
367 sufficiently to yield nitrogen oxide-dominated sulfate production, *Scientific Reports*, 7,
368 12109, doi:12110.11038/s41598-12017-11704-12100, 2017.
- 369 Guo, H., Liu, J., Froyd, K. D., Roberts, J. M., Veres, P. R., Hayes, P. L., Jimenez, J. L., Nenes,
370 A., and Weber, R. J.: Fine particle pH and gas-particle phase partitioning of inorganic
371 species in Pasadena, California, during the 2010 CalNex campaign, *Atmospheric Chemistry*
372 *and Physics*, 17, 5703-5719, 2017.
- 373 Guo, S., Hu, M., Zamora, M. L., Peng, J. F., Shang, D. J., Zheng, J., Du, Z. F., Wu, Z., Shao, M.,
374 Zeng, L. M., Molina, M. J., and Zhang, R. Y.: Elucidating severe urban haze formation in
375 China, *Proceedings of the National Academy of Sciences of the United States of America*,
376 111, 17373-17378, 2014.
- 377 Hung, H.-M., and Hoffman, M. R.: Oxidation of gas-phase SO₂ on the surfaces of acidic
378 microdroplets: Implications for sulfate and sulfate radical anion formation in the
379 atmospheric liquid phase, *Environmental Science & Technology*, 49, 13768-13776, 2015.
- 380 Kawamura, K., and Bikkina, S.: A review of dicarboxylic acids and related compounds in
381 atmospheric aerosols: Molecular distributions, sources and transformation, *Atmospheric*
382 *Research*, 170, 140-160, 2016.
- 383 Khalizov, A.F., Zhang, R., Zhang, D. Xue, H., Pagels, J., and McMurry, P.H.: Formation of
384 highly hygroscopic aerosols upon internal mixing of airborne soot particles with sulfuric
385 acid vapor, *Journal of Geophysical Research-Atmospheres*, 114, D05208,
386 doi:10.1029/2008JD010595, 2009.



- 387 Lee, Y. N., and Schwartz, S. E.: Kinetics of oxidation of aqueous sulfur (IV) by nitrogen
388 dioxide, in Precipitation scavenging, dry deposition, and resuspension, edited by H. R.
389 Pruppacher, R. G. Semmon and W. G. N. Slinn, Elsevier, New York, 1983.
- 390 Li, L., Hoffmann, M. R., and Colussi, A. J.: The role of nitrogen dioxide in the production of
391 sulfate during Chinese haze-aerosol episodes, *Environmental Science & Technology* 52,
392 DOI: 10.1021/acs.est.7b05222, 2018.
- 393 Liu, F., Bi, X., Zhang, G., Peng, L., Lian, X., Lu, H., Fu, Y., Wang, X., Peng, P. a., and Sheng,
394 G.: Concentration, size distribution and dry deposition of amines in atmospheric particles of
395 urban Guangzhou, China, *Atmospheric Environment*, 171, 279-288, 2017.
- 396 Liu, M., Song, Y., Zhou, T., Xu, Z., Yan, C., Zheng, M., Wu, Z., Hu, M., Wu, Y., and Zhu, T.:
397 Fine particle pH during severe haze episodes in Northern China, *Geophysical Research*
398 *Letters*, 44, 5213-5221 ,doi: 5210.1002/2017GL073210, 2017.
- 399 Meng, J., Wang, G., Li, J., Cheng, C., Ren, Y., Huang, Y., Cheng, Y., Cao, J., and Zhang, T.:
400 Seasonal characteristics of oxalic acid and related SOA in the free troposphere of Mt. Hua,
401 central China: Implications for sources and formation mechanisms, *Science of the Total*
402 *Environment*, 493, 1088-1097, 2014.
- 403 Mikhailov, E., Vlasenko, S., Martin, S. T., Koop, T., and Poeschl, U.: Amorphous and crystalline
404 aerosol particles interacting with water vapor: conceptual framework and experimental
405 evidence for restructuring, phase transitions and kinetic limitations, *Atmospheric Chemistry*
406 *and Physics*, 9, 9491-9522, 2009.
- 407 Pagels, J., McMurry, P.H., Khalizov, A.F., and Zhang, R.: Processing of soot by controlled
408 sulphuric acid and water condensation—Mass and mobility relationship, *Aerosol Science &*
409 *Technology*, 43, 629–640, 2009.
- 410 Peng, J., Hu, M., Guo, S., Du, Z., Zheng, J., Shang, D., Zamora, M.L., Zeng, L., Shao, M., Wu,
411 Y., Zheng, J., Wang, Y., Glen, C.R., Collins, D.R., Molina, M.J., and Zhang, R.: Markedly
412 enhanced absorption and direct radiative forcing of black carbon under polluted urban
413 environments, *Proceedings of the National Academy of Sciences of the United States of*
414 *America*, 113, 4266–4271, 2016.
- 415 Peng, C., Chan, M. N., and Chan, C. K.: The hygroscopic properties of dicarboxylic and
416 multifunctional acids: measurements and UNIFAC predictions, *Environmental Science &*
417 *Technology*, 35, 4495-4501, 2001.
- 418 Prenni, A. J., DeMott, P. J., Kreidenweis, S. M., Sherman, D. E., Russell, L. M., and Ming, Y.:
419 The effects of low molecular weight dicarboxylic acids on cloud formation, *Journal of*
420 *Physical Chemistry A*, 105, 11240-11248, 2001.
- 421 Qiu, Q., Wang, L., Lal, V., Khalizov, A.F., and Zhang, R.: Heterogeneous chemistry of
422 Alkylamines on Ammonium Sulfate and Ammonium Bisulfate, *Environmental Science &*
423 *Technology*, 45, 4748–4755, 2011.
- 424 Qiu, C., and Zhang, R.: Physicochemical Properties of Alkylammonium Sulfates: Hygroscopicity,
425 Thermostability, and Density, *Environmental Science & Technology*, 46, 4474-4480, 2012.
- 426 Qiu, C., and Zhang, R. Y.: Multiphase chemistry of atmospheric amines, *Physical Chemistry*
427 *Chemical Physics*, 15(16), 5738-5752, 2013.
- 428 Seinfeld, J. H., and Pandis, S. N., *Atmospheric Chemistry and Physics: From Air Pollution to*
429 *Climate Change, 2nd ed.*, John Wiley & Sons, Hoboken, NJ, 2006.
- 430 Silvern, R.F., Jacob, D.J., Kim, P.S., Marais, E.A., Turner, J. R., Campuzano-Jost, P., and
431 Jimenez, J. L. Inconsistency of ammonium–sulfate aerosol ratios with thermodynamic
432 models in the eastern US: a possible role of organic aerosol, *Atmospheric Chemistry and*



- 433 Physics, 17, 5107–5118, 2017.
- 434 Song, S., Gao, M., Xu, W., Shao, J., Shi, G., Wang, S., Wang, Y., Sun, Y., and McElroy, M. B.:
435 Fine particle pH for Beijing winter haze as inferred from different thermodynamic
436 equilibrium models, Atmospheric Chemistry and Physics Discussions,
437 <https://doi.org/10.5194/acp-2018-6>, 2018.
- 438 Sun, Y. L., Wang, Z. F., Fu, P. Q., Yang, T., Jiang, Q., Dong, H. B., Li, J., and Jia, J. J.: Aerosol
439 composition, sources and processes during wintertime in Beijing, China, Atmospheric
440 Chemistry and Physics, 13(9), 4577–4592, 2013.
- 441 Wang, G., Xie, M., Hu, S., Tachibana, E., and Kawamura, K.: Dicarboxylic acids, metals and
442 isotopic compositions of C and N in atmospheric aerosols from inland China: Implications
443 for dust and coal burning emission and secondary aerosol formation, Atmospheric
444 Chemistry and Physics, 10, 6087–6096, 2010.
- 445 Wang, G., Kawamura, K., Umemoto, N., Xie, M., Hu, S., and Wang, Z.: Water-soluble organic
446 compounds in PM_{2.5} and size-segregated aerosols over Mt. Tai in North China Plain,
447 Journal of Geophysical Research-Atmospheres, 114, D19208,
448 doi:10.1029/2008JD011390, 2009.
- 449 Wang, G., Kawamura, K., Cao, J., Zhang, R., Cheng, C., Li, J., Zhang, T., Liu, S., and Zhao, Z.:
450 Molecular distribution and stable carbon isotopic composition of dicarboxylic acids,
451 ketocarboxylic acids and α -dicarbonyls in size-resolved atmospheric particles from Xi'an
452 city, China, Environmental Science & Technology, 46, 4783–4791, 2012.
- 453 Wang, G., Zhang, R., Zamora, M. L., Gomez, M. E., Yang, L., Hu, M., Lin, Y., Guo, S., Meng,
454 J., Li, J., Cheng, C., Hu, T., Ren, Y., Wang, Y., Gao, J., Cao, J., An, Z., Zhou, W., Jiayuan
455 Wang, Marrero-Ortiz, W., Tian, P., Secret, J., Peng, J., Du, Z., Jing Zheng, Shang, D., Zeng,
456 L., Shao, M., Wang, W., Huang, Y., Wang, Y., Zhu, Y., Li, Y., Hu, J., Pan, B., Cai, L.,
457 Cheng, Y., Rosenfeld, D., Liss, P. S., Duce, R. A., Kolb, C. E., and Molina, M. J.: Persistent
458 Sulfate Formation from London Fog to Chinese Haze, Proceedings of National Academy of
459 Science of United States of America, 113(48), 13630–13635,
460 doi:10.1073/pnas.1616540113., 2016.
- 461 Wang, G. H., Niu, S. L., Liu, C., and Wang, L. S.: Identification of dicarboxylic acids and
462 aldehydes of PM₁₀ and PM_{2.5} aerosols in Nanjing, China, Atmospheric Environment,
463 36(12), 1941–1950, 2002.
- 464 Wang, G. H., Kawamura, K., Watanabe, T., Lee, S. C., Ho, K. F., and Cao, J. J.: Heavy loadings
465 and source strengths of organic aerosols in China, Geophysical Research Letters, 33,
466 L22801, doi:10.1029/2006GL027624, 2006.
- 467 Wang, G. H., Zhou, B. H., Cheng, C. L., Cao, J. J., Li, J. J., Meng, J. J., Tao, J., Zhang, R. J., and
468 Fu, P. Q.: Impact of Gobi desert dust on aerosol chemistry of Xi'an, inland China during
469 spring 2009: differences in composition and size distribution between the urban ground
470 surface and the mountain atmosphere, Atmospheric Chemistry and Physics, 13(2), 819–835,
471 2013.
- 472 Wang, J., Wang, G., Gao, J., Wang, H., Ren, Y., Li, J., Zhou, B., Wu, C., Zhang, L., Wang, S.,
473 and Chai, F.: Concentrations and stable carbon isotope compositions of oxalic acid and
474 related SOA in Beijing before, during, and after the 2014 APEC, Atmospheric Chemistry
475 and Physics, 17(2), 981–992, 2017.
- 476 Wang, L., Lal, V., Khalizov, A.F., and Zhang, R.: Heterogeneous chemistry of alkylamines with
477 sulfuric acid: Implications for atmospheric formation of alkylammonium sulfates,
478 Environmental Science & Technology, 44, 2461–2465, 2010a.



- 479 Wang, L., Khalizov, A.F., Zheng, J., Xu, W., Lal, V., Ma, Y., and Zhang, R.: Atmospheric
480 nanoparticles formed from heterogeneous reactions of organics, *Nature Geoscience*, 3, 238-
481 242, 2010b.
- 482 Wang, Y., Zhang, Q., Jiang, J., Zhou, W., Wang, B., He, K., Duan, F., Zhan, Q., Philip, S., and
483 Xie, Y.: Enhanced sulfate formation during China's severe winter haze episode in January
484 2013 missing from current models, *Journal Geophysical Research-Atmospheres*, 119(17),
485 10425-10440, doi:10.1029/2013JD021426, 2014.
- 486 Wexler, A.S., and Clegg, S. L.: Atmospheric aerosol models for systems including the ions H⁺,
487 NH₄⁺, Na⁺, SO₄²⁻, NO₃⁻, Cl⁻, Br⁻ and H₂O. *Journal of Geophysical Research*, 107
488 (D14), 4207, doi:10.1029/2001JD000451, 2002.
- 489 Yao, L., Wang, M.-Y., Wang, X.-K., Liu, Y.-J., Chen, H.-F., Zheng, J., Nie, W., Ding, A.-J.,
490 Geng, F.-H., Wang, D.-F., Chen, J.-M., Worsnop, D. R., and Wang, L.: Detection of
491 atmospheric gaseous amines and amides by a high-resolution time-of-flight chemical
492 ionization mass spectrometer with protonated ethanol reagent ions, *Atmospheric Chemistry
493 and Physics*, 16(22), 14527-14543, 2016.
- 494 Zhang, R., Wang, G., Guo, S., Zamora, M. L., Ying, Q., Lin, Y., Wang, W., Hu, M., and Wang,
495 Y.: Formation of urban fine particulate matter, *Chemical Reviews*, 115, 3803-3855,
496 doi:10.1021/acs.chemrev.3805b00067, 2015.
- 497 Zhang, H., Chen, S., Zhong, J., Zhang, S., Zhang, Y., Zhang, X., Li, Z., and Zeng, X.C.:
498 Formation of aqueous-phase sulfate during the haze period in China: Kinetics and
499 atmospheric implications, *Atmospheric Environment*, 177, 93-99, 2018.
- 500 Zheng, J., Ma, Y., Chen, M., Zhang, Q., Wang, L., Khalizov, A. F., Yao, L., Wang, Z., Wang, X.,
501 and Chen, L.: Measurement of atmospheric amines and ammonia using the high resolution
502 time-of-flight chemical ionization mass spectrometry, *Atmospheric Environment*, 102, 249-
503 259, 2015.
- 504
505
506

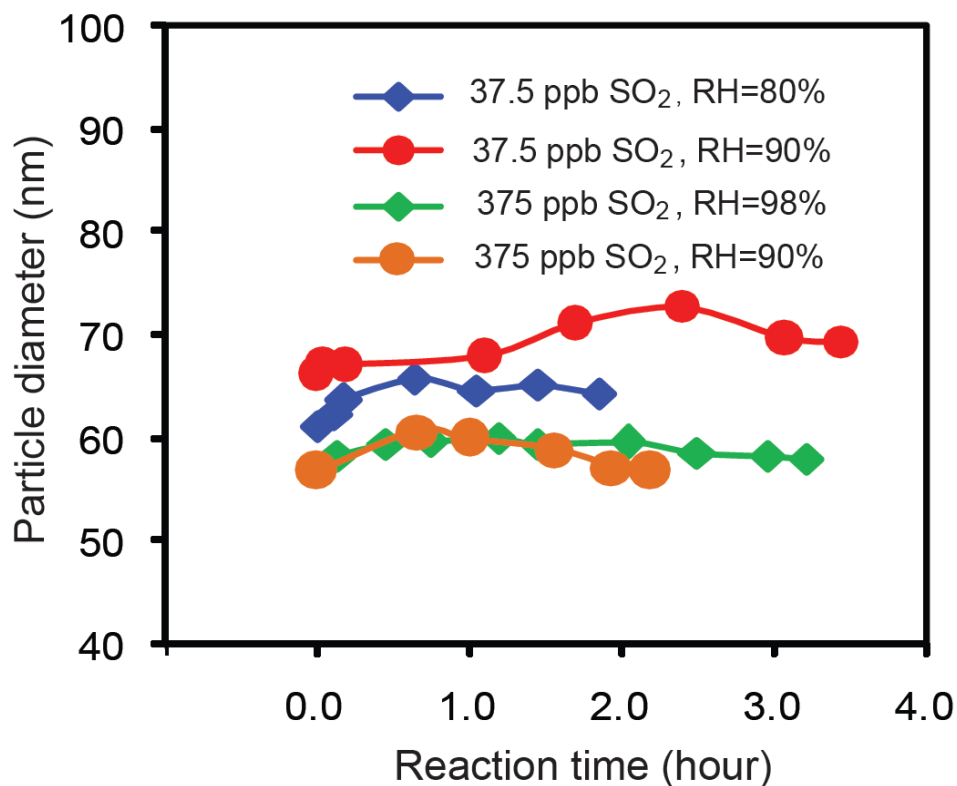
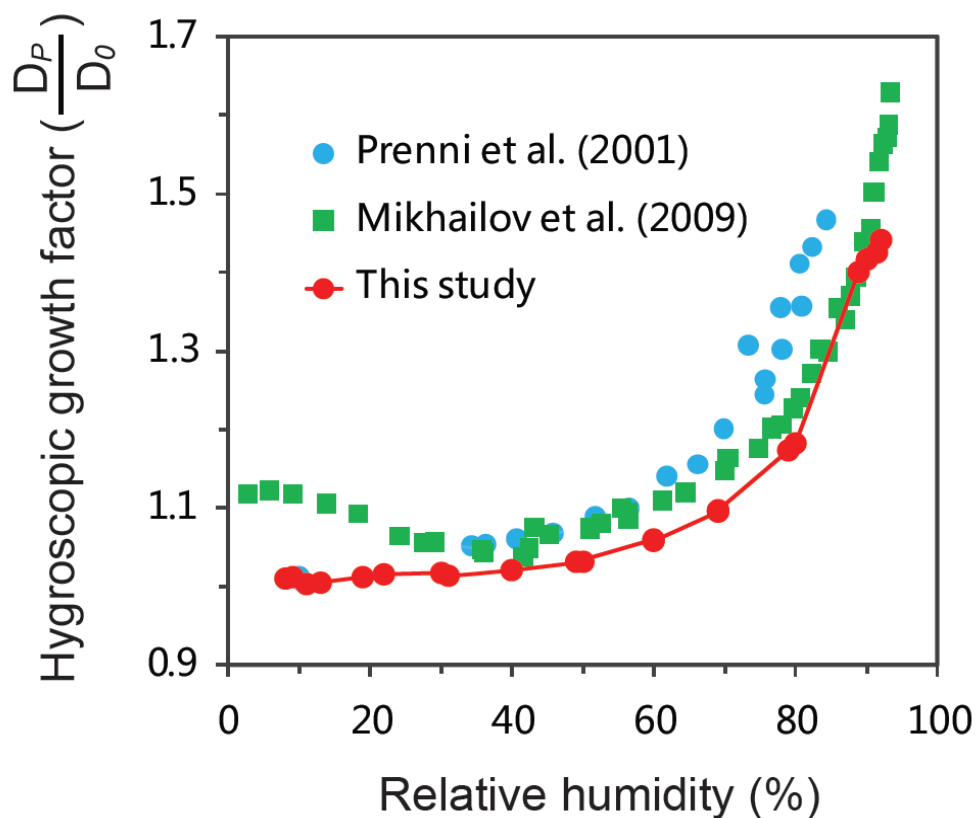
507
508509
510
511
512
513
514
515
516

Figure 1. Size evolution of ammonium sulfate particles after exposure to SO₂, NO₂, and NH₃ at different RH levels. Variations in mobility diameter (D_p) of ammonium sulfate particles as a function of reaction time. The symbols with different colors denote measurements with exposure to different SO₂ concentrations and RH levels. In all cases, the NO₂ concentration is 375 ppb, and the NH₃ concentration is 500 ppb.



517

518



519

520

521

Figure 2. Measured hygroscopic growth factor (HGF) of oxalic acid particles at different RH conditions. D_p is the particle diameter at an elevated RH, and D_0 (100nm) is the initial diameter of oxalic acid particles at RH = 8%.

522

523

524

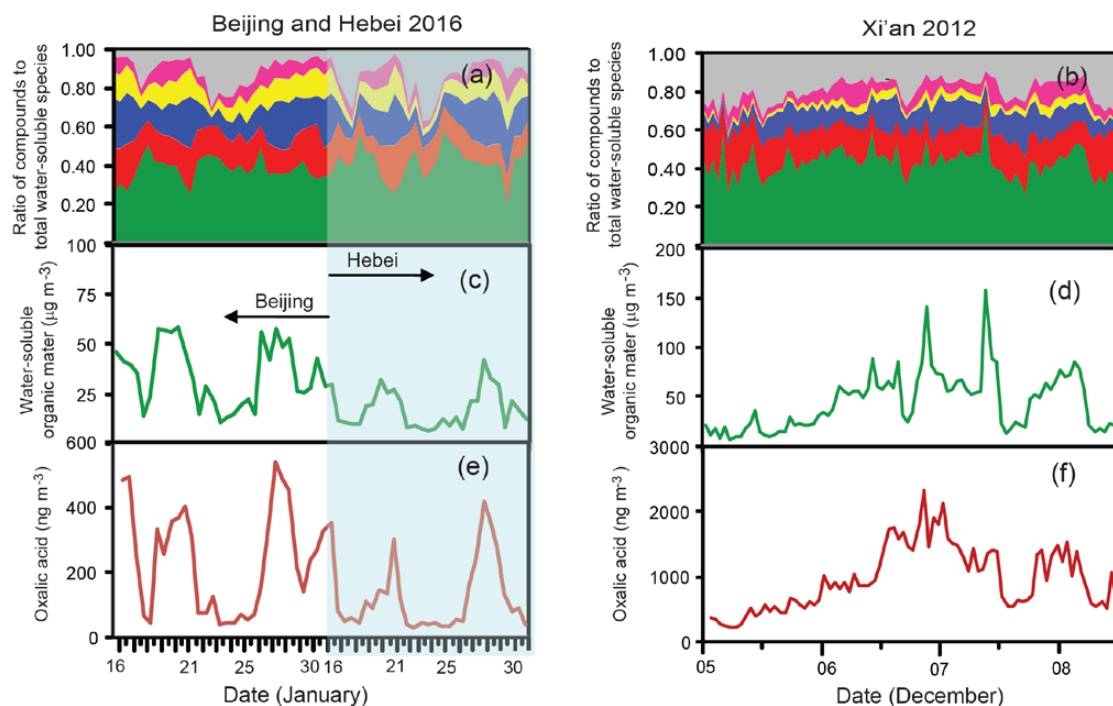
525

526

527

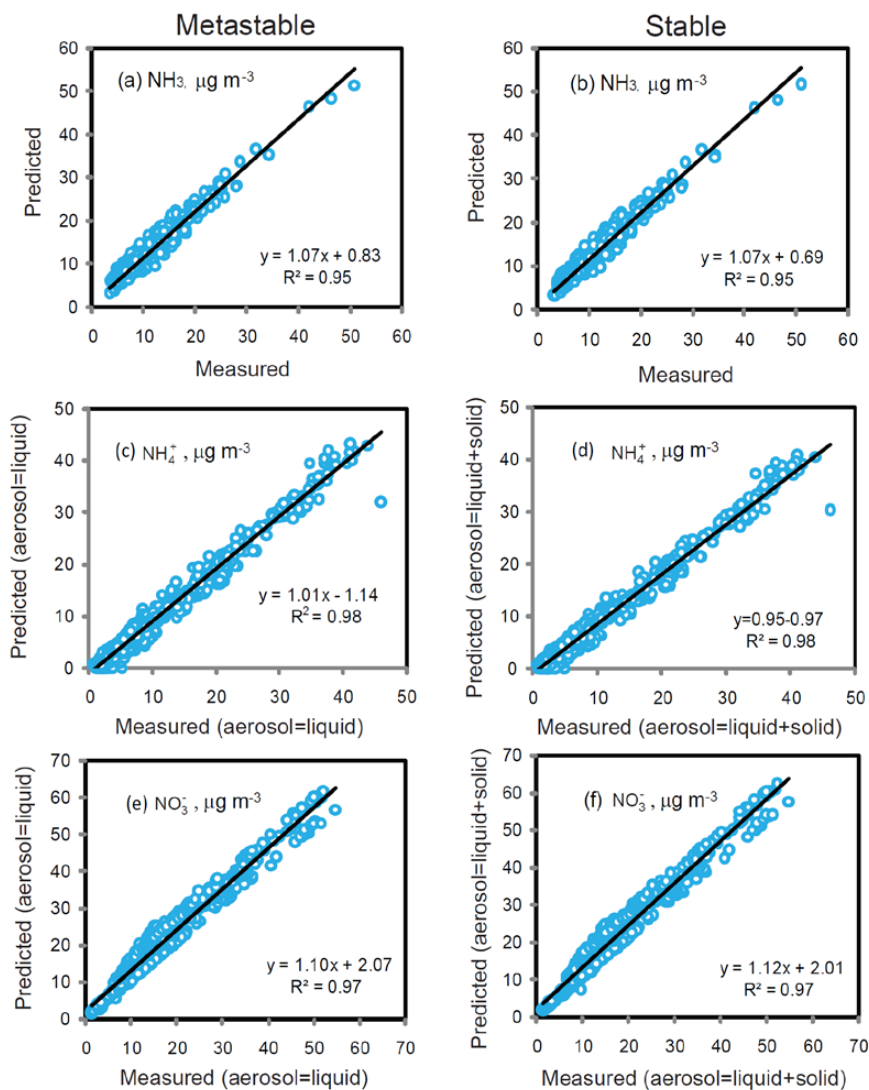
528

529



530
531
532
533
534
535
536

Figure 3. Measurements of water-soluble organic matter (WSOM) of $PM_{2.5}$ collected in Beijing and Hebei Province during the winter of 2016 (left panels: a, c and e) and in Xi'an during the winter of 2012 (right panels: b, d and f). In (a) and (b), the green, red, blue, yellow, pink, and gray colors represent WSOM, sulfate, nitrate, ammonium, chloride, and the others (i.e., the sum of $Na^+ + Ca^{2+} + Mg^{2+} + K^+$), respectively.



537

538 Figure 4. Comparison of measured NH_3 , NH_4^+ , and NO_3^- concentrations with those predicted by
539 ISORROPIA-II model using the forward mode under the metastable (left panels) and stable
540 assumptions (right panels).
541